Whether Kabuki syndrome is the most appropriate diagnosis for the *MLL2* mutation-negative cases is unclear. Some of the *MLL2* mutation-negative cases appear to have a facial phenotype that differs somewhat from that of the *MLL2* mutation-positive cases. Whether these *MLL2* mutation-negative cases diagnosed by expert clinicians should be considered Kabuki syndrome, a variant thereof, or a separate disorder remains to be determined. Our opinion is that there is simply not yet enough information to make an informed decision about this issue.

Most of the mutations in *MLL2* are predicted to result in haploinsufficiency. However, it is unclear by what mechanism(s) haploinsufficiency of *MLL2* could cause Kabuki syndrome. *MLL2* encodes a histone 3 lysine 4 (H3K4) methyltransferase, one of at least 10 proteins (genes for which have not to our knowledge yet been screened in Kaubki cases in which *MLL2* mutations were not found) that have been identified to specifically modify the lysine residue at the fourth amino acid position of the histone H3 protein [Kouzarides, 2007]. MLL2 has a SET domain near its C-terminus that is shared by yeast Set1, *Drosophila* Trithorax (TRX) and human MLL1 [FitzGerald and Diaz, 1999]. MLL2 appears to regulate gene transcription and chromatin structure in early development [Prasad et al., 1997]. In mice, loss of *MLL2* results in embryonic lethality before E10.5, and while $Mll2^{+/-}$ mice are viable, they are smaller than wild type (Kai Ge, personal communication).

Kabuki syndrome is the most common of a small, but growing group of multiple malformation syndromes accompanied by developmental delay that are caused by mutations in genes that encode proteins involved in histone methylation [De Sario, 2009]. The most notable of these is CHARGE syndrome, which is one of the syndromes often considered in the differential diagnosis of children ultimately diagnosed with Kabuki syndrome. CHARGE syndrome is caused by mutations in *CHD7*, which encodes a chromodomain protein that recognizes the trimethylated H3K4 side chain [Vissers et al., 2004]. Other disorders caused by defects of histone methylation status include several intellectual disability syndromes, some of which are also characterized by malformations (e.g., cleft lip/palate) that overlap with those found in individuals with Kabuki syndrome.

Kabuki syndrome is one of the most common causes of heritable developmental delay. Discovery that mutations in *MLL2* are the most common cause of Kabuki syndrome highlights the role that disrupted regulation of histone methylation plays as a cause of human birth defects. Characterizing the spectrum of mutations in *MLL2* is a small but important first step toward understanding the mechanism(s) that underlies Kabuki syndrome.

Supplementary Material

Refer to Web version on PubMed Central for supplementary material.

Acknowledgments

We thank the families for their participation and the Kabuki Syndrome Network for their support. Our work was supported in part by grants from the National Institutes of Health/National Heart Lung and Blood Institute (5R01HL094976 to D.A.N. and J.S.), the National Institutes of Health/National Human Genome Research Institute (5R21HG004749 to J.S., 1RC2HG005608 to M.J.B., D.A.N., and J.S.; and 5RO1HG004316 to H.K.T.), National Institute of Heath/National Institute of Environmental Health Sciences (HHSN273200800010C to D.N. and M.R.), National Institute of Neurological Disorders and Stroke (RO1NS35102 to C.S.M.) NIHR Manchester Biomedical Research Centre (D. D.), Ministry of Health, Labour and Welfare (K.Y., N.M., T.O., and N.N.), Ministry of Health, Labour and Welfare of Japan (N.M), Japan Science and Technology Agency (N.M.), Society for the Promotion of Science (N.M.), the Life Sciences Discovery Fund (2065508 and 0905001), the Washington Research Foundation, and the National Institutes of Health/National Institute of Child Health and Human Development (1R01HD048895 to M.J.B. and 5K23HD057331 to A.E.B.). S.B.N. is supported by the Agency for Science, Technology and Research, Singapore. A.W.B. is supported by a training fellowship from the National Institutes of Health/National Human Genome Research Institute (T32HG00035).

References

Adam MP, Hudgins L. Kabuki syndrome: a review. Clin Genet. 2005; 67(3):209–219. [PubMed: 15691356]

De Sario A. Clinical and molecular overview of inherited disorders resulting from epigenomic dysregulation. Eur J Med Genet. 2009; 52(6):363–372. [PubMed: 19632366]

FitzGerald KT, Diaz MO. MLL2: A new mammalian member of the trx/MLL family of genes. Genomics. 1999; 59(2):187–192. [PubMed: 10409430]

Kouzarides T. Chromatin modifications and their function. Cell. 2007; 128(4):693–705. [PubMed: 17320507]

Kuroki Y, Suzuki Y, Chyo H, Hata A, Matsui I. A new malformation syndrome of long palpebral fissures, large ears, depressed nasal tip, and skeletal anomalies associated with postnatal dwarfism and mental retardation. J Pediatr. 1981; 99(4):570–573. [PubMed: 7277097]

Kurotaki N, Imaizumi K, Harada N, Masuno M, Kondoh T, Nagai T, Ohashi H, Naritomi K, Tsukahara M, Makita Y, Sugimoto T, Sonoda T, Hasegawa T, Chinen Y, Tomita Ha HA, Kinoshita A, Mizuguchi T, Yoshiura Ki K, Ohta T, Kishino T, Fukushima Y, Niikawa N, Matsumoto N. Haploinsufficiency of NSD1 causes Sotos syndrome. Nat Genet. 2002; 30(4):365–366. [PubMed: 11896389]

Ng SB, Bigham AW, Buckingham KJ, Hannibal MC, McMillin MJ, Gildersleeve HI, Beck AE, Tabor HK, Cooper GM, Mefford HC, Lee C, Turner EH, Smith JD, Rieder MJ, Yoshiura K, Matsumoto N, Ohta T, Niikawa N, Nickerson DA, Bamshad MJ, Shendure J. Exome sequencing identifies MLL2 mutations as a cause of Kabuki syndrome. Nat Genet. 2010; 42(9):790–793. [PubMed: 20711175]

Niikawa N, Kuroki Y, Kajii T, Matsuura N, Ishikiriyama S, Tonoki H, Ishikawa N, Yamada Y, Fujita M, Umemoto H, et al. Kabuki make-up (Niikawa-Kuroki) syndrome: a study of 62 patients. Am J Med Genet. 1988; 31(3):565–589. [PubMed: 3067577]

Niikawa N, Matsuura N, Fukushima Y, Ohsawa T, Kajii T. Kabuki make-up syndrome: a syndrome of mental retardation, unusual facies, large and protruding ears, and postnatal growth deficiency. J Pediatr. 1981; 99(4):565–569. [PubMed: 7277096]

Prasad R, Zhadanov AB, Sedkov Y, Bullrich F, Druck T, Rallapalli R, Yano T, Alder H, Croce CM, Huebner K, Mazo A, Canaani E. Structure and expression pattern of human ALR, a novel gene with strong homology to ALL-1 involved in acute leukemia and to Drosophila trithorax. Oncogene. 1997; 15(5):549–560. [PubMed: 9247308]

Vissers LE, van Ravenswaaij CM, Admiraal R, Hurst JA, de Vries BB, Janssen IM, van der Vliet WA, Huys EH, de Jong PJ, Hamel BC, Schoenmakers EF, Brunner HG, Veltman JA, van Kessel AG. Mutations in a new member of the chromodomain gene family cause CHARGE syndrome. Nat Genet. 2004; 36(9):955–957. [PubMed: 15300250]

White SM, Thompson EM, Kidd A, Savarirayan R, Turner A, Amor D, Delatycki MB, Fahey M, Baxendale A, White S, Haan E, Gibson K, Halliday JL, Bankier A. Growth, behavior, and clinical findings in 27 patients with Kabuki (Niikawa-Kuroki) syndrome. Am J Med Genet A. 2004; 127A(2):118–127. [PubMed: 15108197]

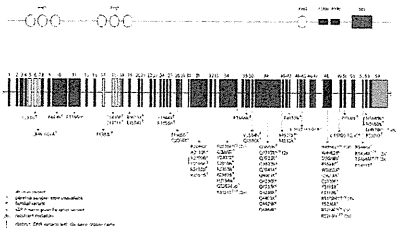

Figure 1. Genomic structure and allelic spectrum of *MLL2* mutations that cause Kabuki syndrome

MLL2 is composed of 54 exons that include untranslated regions (orange) and protein coding sequence (blue) including 7 PHD fingers (yellow), FYRN (green), FYRC (green), and a SET domain (red). Arrows indicate the locations of 81 mutations affecting 70 sites found in 110 families with Kabuki syndrome including: 37 nonsense, 22 frameshifts, 16 missense, 3 in-frame deletions/duplications, and 3 splice-site mutations. Asterisks indicate mutations that were confirmed to be *de novo* and crosses indicate cases for which parental DNA was unavailable.

Figure 2.
Facial photographs of mother and daughter with Kabuki syndrome in whom no causative mutation in *MLL2* was identified. Both have mild developmental delay and no known major malformations.

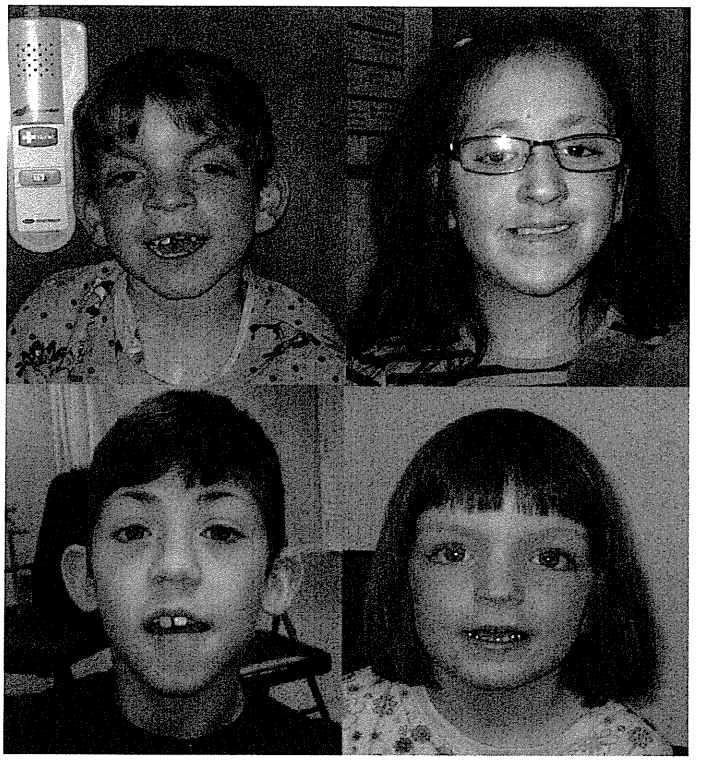

Figure 3.
Facial photographs of four children diagnosed with Kabuki syndrome in whom no causative mutation in *MLL2* was found.

Table I

Phenotypic traits grouped by *MLL2* mutation status (a) and type (b)

Trait	***MLL2*+**	***MLL2*−**
Intellectual Disability	74/74 (100%)	19/20 (95%)
Mild	51/74 (69%)	10/20 (50%)
Moderate	18/74 (24%)	4/20 (20%)
Severe	4/74 (5%)	3/20 (15%)
Cleft palate, CL/CP	29/72 (40%)	8/18 (44%)
Congenital heart defect	36/71 (51%)	8/19 (42%)
Renal abnormality	31/66 (47%)	2/14 (14%)
Trait	**Truncating (N=59)**	**Missense (N=16)**
Intellectual disability	54/54 (100%)	15/15 (100%)
Mild	36/54 (67%)	11/15 (73 %)
Moderate	13/54 (24%)	4/15 (27%)
Severe	5/54 (9%)	0/15
Cleft palate, CL/CP	23/54 (43%)	3/14 (21%)
Congenital heart defect	30/54 (55%)	4/13 (30%)
Renal anomaly	9/44 (20%)	2/12 (17%)

CLINICAL GENETICS An International Journal of Genetics, Molecular and Personalized Medicine

Clin Genet 2011: 80: 161–166
Printed in Singapore. All rights reserved

CLINICAL GENETICS
doi: 10.1111/j.1399-0004.2011.01721.x

Short Report

Exome sequencing of two patients in a family with atypical X-linked leukodystrophy

Tsurusaki Y, Okamoto N, Suzuki Y, Doi H, Saitsu H, Miyake N, Matsumoto N. Exome sequencing of two patients in a family with atypical X-linked leukodystrophy.
Clin Genet 2011: 80: 161–166. © John Wiley & Sons A/S, 2011

We encountered a family with two boys similarly showing brain atrophy with reduced white matter, hypoplasia of the brain stem and corpus callosum, spastic paralysis, and severe growth and mental retardation without speaking a word. The phenotype of these patients was not compatible with any known type of syndromic leukodystrophy. Presuming an X-linked disorder, we performed next-generation sequencing (NGS) of the transcripts of the entire X chromosome. A single lane of exome NGS in each patient was sufficient. Six potential mutations were found in both affected boys. Two missense mutations, including c.92T>C (p.V31A) in *L1CAM*, were potentially pathogenic, but this remained inconclusive. The other four could be excluded. Because the patients did not show adducted thumbs or hydrocephalus, the *L1CAM* change in this family can be interpreted as different scenarios. Personal genome analysis using NGS is certainly powerful, but interpretation of the data can be a substantial challenge requiring a lot of tasks.

Conflict of interest

None of the authors have any conflicts of interest to disclose.

Y Tsurusaki[a], N Okamoto[b], Y Suzuki[c], H Doi[a], H Saitsu[a], N Miyake[a] and N Matsumoto[a]

[a]Department of Human Genetics, Yokohama City University Graduate School of Medicine, Kanazawa-ku, Yokohama, Japan, and [b]Department of Medical Genetics, and [c]Department of Pediatric Neurology, Osaka Medical Center and Research Institute for Maternal and Child Health; Murodo-cho, Izumi, Japan

Key words: atypical phenotype – exome sequencing – *L1CAM* – X-linked leukodystrophy

Corresponding author: Naomichi Matsumoto, Department of Human Genetics, Yokohama City University Graduate School of Medicine, 3-9 Fukuura, Kanazawa-ku, Yokohama 236-0004, Japan.
Tel.: +81-45-787-2606;
fax: +81-45-786-5219;
e-mail: naomat@yokohama-cu.ac.jp

Received 4 May 2011, revised and accepted for publication 31 May 2011

Focused/selected gene and genomic characterization has usually been carried out in clinically homogeneous groups of multiple affected samples to make identification of genetic abnormalities more efficient. Microarrays and next-generation sequencing (NGS) have provided new avenues for human genetic research (1–6). Using such new technologies, researchers are able to analyze small numbers of patients on a genome-wide scale. Even very rare cases (such as when only a few compatible patients are available or atypical patients showing no similar phenotypes) can be realistic targets of genetic research, as the new technologies can identify aberrations in a single gene from within virtually the whole genome; this could not be achieved with conventional techniques.

We encountered a family with two affected males showing atypical leukodystrophy. The phenotype of these patients did not match any known type of syndromic leukodystrophy. Because we presumed that abnormality of an X-linked gene caused the atypical leukodystrophy in this family, we performed exome sequencing of most of the X-chromosome transcripts and identified an unexpected gene mutation in these patients.

Materials and methods

A family with atypical X-linked leukodystrophy

Two brothers, II-1 currently aged 19 years and II-2 currently aged 17 years, who have unrelated healthy parents, presented with similar clinical

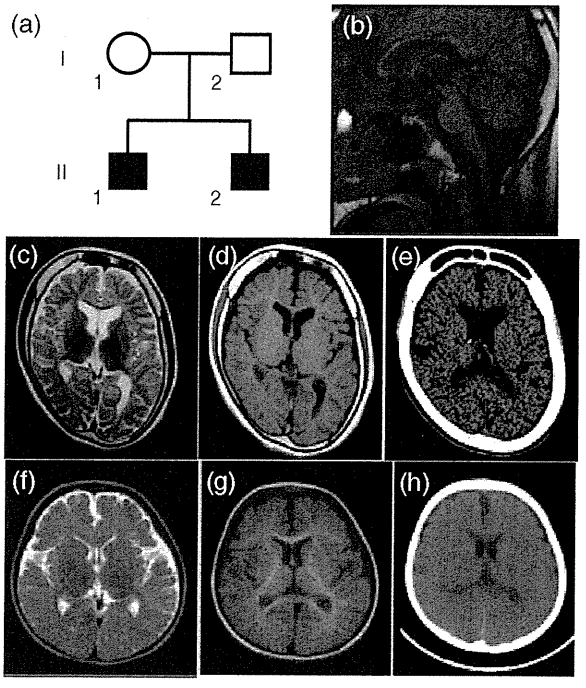

Fig. 1. Clinical features of the family. Familial pedigree (**a**). Brain magnetic resonance imaging (MRI) (**b**: T1-weighted image, **c**: T2-weighted image, **d**: T1-weighted image) of individual II-1 at 16 years old showing hypoplasia of the white matter, the brain stem and the corpus callosum. Brain computed tomographic (CT) images of individual II-1 at 19 years old (**e**) indicating a thick calvarium with enlarged frontal sinus as well as calcification of the choroid plexus in the atrophic brain. Brain MRI (**f**: T2-weighted image, **g**: T1-weighted image) of individual II-2 at 2 years old, also displaying hypoplasia of the white matter. Brain CT image of individual II-2 at 5 years old (**h**), also showing a thick calvarium.

features. Their mother did not show any neurological abnormalities (Fig. 1a).

Patient II-1

Patient II-1's birth weight was 2840 g at 40 weeks of gestational age. He had congenital nystagmus. He sat unsupported at 7 months old but after this his developmental milestones were delayed. He could creep at 18 months old. Spastic paralysis, especially in the lower extremities, became apparent. He was unable to stand unsupported. His mental development was severely delayed, and he needed special education from elementary school. He had suffered generalized epileptic seizures since he was 10 years old. He was confined to a wheelchair. He had severe mental retardation without speaking a word. His developmental quotient (DQ) at 9 years old was 19 by the Japanese standard method. Severe growth retardation [143 cm (<3%), 24 kg (<3%), occipitofrontal head circumference 49 cm (<3%) at 19 years] was also noted. He did not have dysmorphic features. Blood analysis revealed microcytic anemia [hemoglobin (Hb) 13.4 g/dl, mean corpuscular volume (MCV) (of red blood cell) 70.4 fl (normal: 89–99 fl), mean corpuscular hemoglobin (MCH) (of red blood cell) 23.1 pg (normal: 29–35 pg)] without any evidence of hemolysis or iron deficiency. Hormonal examination indicated that the levels of luteinizing hormone, follicle-stimulating hormone, and thyroid-stimulating hormone were all low [0.9 mIU/ml (normal: 1.2–8.0 mIU/ml), 2.5 mIU/ml (normal: 2.3–15.1 mIU/ml), <0.01 μIU/ml (normal: 0.5–5.0 μIU/ml), respectively]. He showed delayed puberty with small testes. Pubic hair only appeared at 17 years old. His bone age at 18 years old was 12.6 years (67%). Brain magnetic resonance imaging (MRI) at 16 years old revealed brain atrophy associated with reduced white matter and hypoplasia of the brain stem and the corpus callosum (Fig. 1b–d). No hydrocephalus or adducted thumb was observed. Brain computed tomography (CT) at 19 years old showed a thick calvarium with enlarged frontal sinus as well as calcification of the cerebellar tentorium and the choroid plexus (Fig. 1e).

Patient II-2

Patient II-2's birth weight was 2910 g at 37 weeks of gestational age. Developmental delay was apparent since he was 10 months old. Spastic paralysis (especially in the lower extremities), confinement to a wheelchair, severe mental retardation without speaking a word (DQ = 5 at 17 years old), and severe growth retardation [130 cm (<3%) and 27 kg (<3%) at 17 years] were phenotypes shared with his brother (II-1). Blood analysis revealed microcytic anemia (Hb 12.0 g/dl, MCV 61.1 fl, MCH 19.0 pg) without any evidence of hemolysis or iron deficiency. Hormonal examination indicated that the levels of luteinizing hormone, follicle-stimulating hormone, and thyroid-stimulating hormone were relatively low (1.9 mIU/ml, 4.2 mIU/ml, <0.23 μIU/ml, respectively). He also showed delayed puberty with small testes. Pubic hair appeared only at 17 years old. His bone age at 17 years old was 11 years (65%). Brain MRI at 2 years old revealed brain atrophy associated with reduced white matter and hypoplasia of the brain stem and corpus callosum (Fig. 1f,g). Brain CT at 5 years old showed a thick calvarium (Fig. 1h). No hydrocephalus or adducted thumb was observed. Most of the clinical features were similar to those of his brother except for the absence of nystagmus in patient II-2.

Genome-wide SNP genotyping

Genome-wide single-nucleotide polymorphism (SNP) genotyping was performed on individuals I-2, II-1, and II-2 using a GeneChip™ Human Mapping 10K Array Xba 142 2.0 (Affymetrix, Inc., Santa Clara, CA), according to the manufacturer's protocols. Mendelian error in the pedigree to exclude conflicted SNPs was checked using GCOS 1.2 (GeneChip Operating Software; Affymetrix) and batch analysis in GTYPE 4.0 (GeneChip Genotyping Analysis Software; Affymetrix), with the default setting for the mapping algorithm. The linked region, with SNP genotypes shared between individuals II-1 and II-2, was checked manually.

Genomic partitioning, short-read sequencing, and sequence alignment

Three micrograms of genomic DNA from the affected brothers (II-1 and II-2) was processed using a SureSelect X Chromosome test kit (1582 transcripts covering 3053 kb) (Agilent Technologies, Santa Clara, CA), according to the manufacturer's instructions. Captured DNAs were analyzed using an Illumina GAIIx (Illumina, Inc., San Diego, CA). We used only one of the eight lanes in the flow cell (Illumina) for paired-end, 76-bp reads per sample. Image analysis and base-calling were performed using sequence control software (SCS) real-time analysis and off-line BASECALLER software v1.8.0 (Illumina). Reads were aligned to the human reference genome (UCSC hg19, NCBI build 37.1) using the ELANDv2 algorithm in CASAVA_v1.7.0 (Illumina). The ELANDv2 algorithm can align 100-bp reads to a reference sequence and split the reads into multiple seeds.

Mapping strategy and variant annotation

Approximately 57.5 million reads from individual II-1 and 71.1 million reads from individual II-2 that passed the quality control (Path Filter) were mapped to the human reference genome using mapping and assembly with quality (MAQ) (7) (Fig. 2). MAQ was able to align 51 720 952 and 65 990 660 reads to the whole genome for individuals II-1 and II-2, respectively; these were then statistically analyzed for coverage using a script created by BITS Co., Ltd. (Tokyo, Japan). SNPs and insertions/deletions were extracted from the alignment data using an original script created by BITS Co., Ltd., along with information on the registered SNPs (dbSNP 131). A consensus quality score of 40 or more was used for the SNP analysis in MAQ. SNPs in MAQ-passed reads were annotated using the SeattleSeq website (http://gvs.gs.washington.edu/SeattleSeqAnnotation/). Variants found by each informatics method were selected in terms of location on chromosome X, unregistered variants (excluding registered SNPs), variants in known genes, variants in coding regions, variants excluding synonymous changes, and variants with an allele frequency of at least 90% (assuming a homozygous mutation). NEXTGENE software v2.0 (SoftGenetics, State College, PA) was also used to analyze the reads, with a default setting. Variants found by both of the informatics methods were selected. The variants found in common between individuals II-1 and II-2 were focused on, and confirmed as true positives by Sanger sequencing of polymerase chain reaction (PCR) products amplified from patient genomic DNA, except for variants within genes at segmental duplications. The pathological significance of the variants was evaluated using four different websites: POLYPHEN (Polymorphism Phenotyping; http://genetics.bwh.harvard.edu/pph/index.html), POLYPHEN-2 (http://genetics.bwh.harvard.edu/pph2/index.shtml), SIFT (http://sift.jcvi.org/) (output values less than 0.05 are deleterious), and MUTATIONTASTER (http://neurocore.charite.de/MutationTaster/).

Capillary sequencing

Possible pathological variants were confirmed by Sanger sequencing using an ABI 3500xl or ABI3100 autosequencer (Life Technologies, Carlsbad, CA), following the manufacturer's protocol. Sequencing data were analyzed using SEQUENCHER software (Gene Codes Corporation, Ann Arbor, MI).

Expression studies

The relative mRNA levels of *TMEM187* in cDNA of various fetal and adult human tissues (Human MTC™ Panel I and Human Fetal MTC™ Panel; Clontech, Mountain View, CA) were determined by quantitative real-time reverse transcription–polymerase chain reaction (RT-PCR) using TaqMan gene expression assays (Hs01920894_s1 for *TMEM187* and Hs00357333_g1 for β-actin as a control) (Life Technologies).

Results and discussion

Our coverage analysis indicated that for individuals II-1 and II-2, 79.2% and 78.8%, respectively, of the entire X-chromosome coding sequence (CDS) were completely covered, and 88.5% and 88.5%,

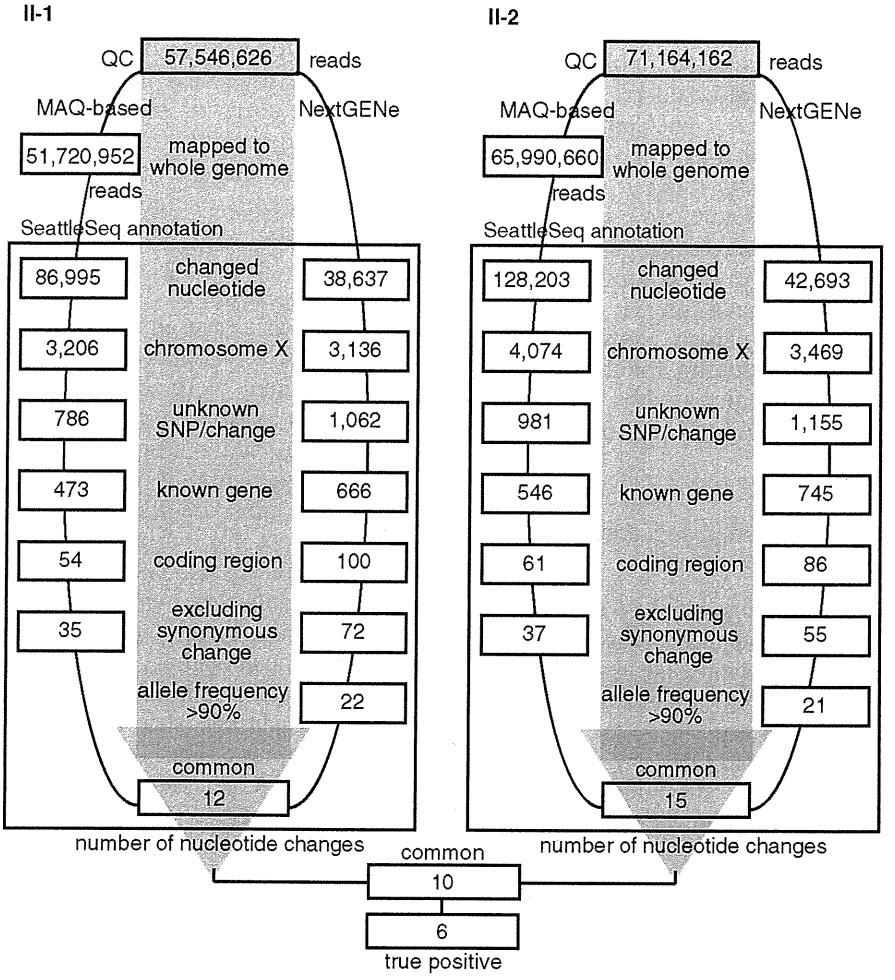

Fig. 2. Flow of informatics analysis. A MAQ-based method and NextGENe analysis were performed in individuals II-1 and II-2. The selection methods employed included variants compared with the human genome reference sequence, variants mapped to chromosome X, unknown variants [excluding registered single-nucleotide polymorphisms (SNPs)], variants in known genes, variants in coding regions, variants excluding synonymous changes, and variants common to the two informatics methods. Finally, the nucleotide changes in common between individuals II-1 and II-2 were focused on as potentially pathogenic mutations. True positive changes were confirmed by capillary sequencing of polymerase chain reaction (PCR) products amplified from genomic DNA.

respectively, of the CDS were at least 90% covered by reads. Using a single lane of sequencing per sample, the coverage with 20 reads or more comprised 89.6% and 89.7% of the CDS, and that with 100 reads or more comprised 87.6% and 89.7% of the CDS in individuals II-1 and II-2, respectively. SNP genotyping indicated that the region from rs727240 to rs721003 (UCSC genome browser hg19 assembly, chromosome X coordinates: 22131639–54454152; 32.2 Mb) was unlinked to the phenotype. Exome sequencing using two informatics methods successfully identified six potentially interesting changes as true positives in the linked region: *FAM123B* (RefSeq Gene ID NM_152424): c.85G>A (p.A29T), *FRMD7* (NM_194277): c.875T>C (p.L292P), *L1CAM* (NM_000425): c.92T>C (p.V31A), *TMEM187* (NM_003492): c.334G>A (p.A112T), *FLNA* (NM_001110556): c.1582G>A (p.V528M), and *LAGE3* (NM_006014): c.395G>A (p.R132Q).

The c.92T>C (p.V31A) variant in *L1CAM* was previously found in a patient with Hirschsprung disease, acrocallosal syndrome, and congenital hydrocephalus (8). *L1CAM* mutations cause a wide variety of clinical phenotypes: hydrocephalus due to stenosis of the aqueduct of Sylvius (MIM #307000), MASA syndrome (mental retardation, aphasia, shuffling gait, adducted thumb; MIM #303350), and X-linked agenesis of the corpus callosum (MIM #217990). Phenotypic variability, even within a family, has been noted, raising the caution that definite clinical diagnosis in single

Table 1. Characterization of nucleotide changes found by exome sequencing

	FAM123B	*FRMD7*	*L1CAM*	*TMEM187*	*FLNA*	*LAGE3*
Change	c.85G>A (p.A29T)	c.875T>C (p.L292P)	c.92T>C (p.V31A)	c.334G>A (p.A112T)	c.1582G>A (p.V528M)	c.395G>A (p.R132Q)
PolyPhen	Benign	Probably damaging	Benign	Benign	Possibly damaging	Benign
PolyPhen-2	Probably damaging	Probably damaging	Benign	Possibly damaging	Possibly damaging	Possibly damaging
SIFT	0.04	0.02	0.22	0.02	0.04	0.46
MutationTaster	Polymorphism	Disease causing	Disease causing	Polymorphism	Polymorphism	Polymorphism
Normal female	8/502[a]	2/502	2/502	1/502	15/502[a]	4/502
Normal male	1/118	0/117	0/118	0/118		1/86
Note		No nystagmus in II-2				

[a]Including one homozygous female. Underlining means that this result excludes the variant as potentially causative. Grayed shading indicates the variants that could not be excluded; between these two, the *L1CAM* variant is more likely to be causative.

cases is often impossible (9). Phenotypic features compatible with the *L1CAM* mutation in our patients include spastic paralysis, aphasia, severe mental and growth retardation, but atypical leukodystrophy and the absence of adducted thumbs were very rare or exceptional (9). A normal control study found that 2 of 251 normal females were heterozygous for this SNP, but none of 117 normal males carried the variant allele. One of the four web-based analyses of pathological significance (MutationTaster) indicated that this variant would be disease causing, while the others indicated that it would be benign (Table 1). X-linked hydrocephalus due to *L1CAM* mutations occurs in approximately 1/30 000 male births (10). Considering that the *L1CAM* mutation was found in 2/618 control alleles (0.32%), the change may be a rare polymorphism, a mutation causing lethality in the majority of affected males, or a mutation with low penetrance. Because we were unable to exclude this *L1CAM* change, its pathogenic status remains inconclusive.

We next examined c.85G>A in *FAM123B*, c.875T>C in *FRMD7*, c.1582G>A in *FLNA*, and c.395G>A in *LAGE3* in normal controls. The *FAM123B*, *FLNA*, and *LAGE3* variants were excluded as causative because a homozygous change was found in 1 of 251 female controls (*FAM123B* and *FLNA*) or a hemizygous change was found in 1 of 86 normal males (*LAGE3*). However, the thick calvarium in individuals II-1 and II-2 may be influenced by the *FAM123B* change, because it is causative for osteopathia striata with cranial sclerosis, an X-linked dominant disorder (MIM #300373) (11, 12). As the calvarium of the patients' mother having the heterozygous *FAM123B* change was not evaluated by CT, we could not confirm this possibility.

Only 2 of 251 control females carried the c.875T>C variant in *FRMD7* heterozygously, and none of 117 male controls carried this variant; thus, the pathogenicity of the *FMRD7* variant was inconclusive. Other *FRMD7* mutations cause X-linked congenital nystagmus 1 (MIM #310700) (13). However, the nystagmus found in individual II-1 was not observed in individual II-2, indicating that the variant in common between two brothers did not consistently cause nystagmus. Thus, it may not contribute to the phenotype in this family (Table 1).

We also evaluated the c.334G>A variant in *TMEM187*. Only 2 of 251 female controls carried this heterozygous change, and it was not found among 118 male controls. Two of the four programs (PolyPhen-2 and SIFT) indicated that it would be pathogenic. By Taqman assay, *TMEM187* was ubiquitously expressed in various fetal and adult tissues, including the brain (data not shown), leaving the effect of this mutation on the phenotype in these patients inconclusive (Table 1).

In conclusion, we found two possible but inconclusive variants in this family with two boys affected by atypical leukodystrophy. High-throughput technologies are clearly powerful to detect genomic changes, but evaluation of the data can be very difficult and should be performed cautiously. More knowledge of rare SNPs and mutations is absolutely necessary before any conclusions can be drawn.

Acknowledgements

We would like to thank the patients and their family members for their participation in this study. This work was supported by research grants from the Ministry of Health, Labour and Welfare

(to H. S., N. Miyake, and N. Matsumoto), the Japan Science and Technology Agency (to N. Matsumoto), a Grant-in-Aid for Scientific Research from the Japan Society for the Promotion of Science (to N. Matsumoto), and a Grant-in-Aid for Young Scientists from the Japan Society for the Promotion of Science (to H. D., N. Miyake, and H. S.).

References

1. Saitsu H, Kato M, Mizuguchi T et al. De novo mutations in the gene encoding STXBP1 (MUNC18-1) cause early infantile epileptic encephalopathy. Nat Genet 2008: 40: 782–788.
2. Check Hayden E. Genomics shifts focus to rare diseases. Nature 2009: 461: 458.
3. Biesecker LG. Exome sequencing makes medical genomics a reality. Nat Genet 2010: 42: 13–14.
4. Kuhlenbaumer G, Hullmann J, Appenzeller S. Novel genomic techniques open new avenues in the analysis of monogenic disorders. Hum Mutat 2011: 32: 144–151.
5. Miyake N, Kosho T, Mizumoto S et al. Loss-of-function mutations of CHST14 in a new type of Ehlers-Danlos syndrome. Hum Mutat 2010: 31: 966–974.
6. Ng SB, Bigham AW, Buckingham KJ et al. Exome sequencing identifies MLL2 mutations as a cause of Kabuki syndrome. Nat Genet 2010: 42: 790–793.
7. Li H, Ruan J, Durbin R. Mapping short DNA sequencing reads and calling variants using mapping quality scores. Genome Res 2008: 18: 1851–1858.
8. Nakakimura S, Sasaki F, Okada T et al. Hirschsprung's disease, acrocallosal syndrome, and congenital hydrocephalus: report of 2 patients and literature review. J Pediatr Surg 2008: 43: E13–E17.
9. Rietschel M, Friedl W, Uhlhaas S, Neugebauer M, Heimann D, Zerres K. MASA syndrome: clinical variability and linkage analysis. Am J Med Genet 1991: 41: 10–14.
10. Rosenthal A, Jouet M, Kenwrick S. Aberrant splicing of neural cell adhesion molecule L1 mRNA in a family with X-linked hydrocephalus. Nat Genet 1992: 2: 107–112.
11. Viot G, Lacombe D, David A et al. Osteopathia striata cranial sclerosis: non-random X-inactivation suggestive of X-linked dominant inheritance. Am J Med Genet 2002: 107: 1–4.
12. Jenkins ZA, van Kogelenberg M, Morgan T et al. Germline mutations in WTX cause a sclerosing skeletal dysplasia but do not predispose to tumorigenesis. Nat Genet 2009: 41: 95–100.
13. Tarpey P, Thomas S, Sarvananthan N et al. Mutations in FRMD7, a newly identified member of the FERM family, cause X-linked idiopathic congenital nystagmus. Nat Genet 2006: 38: 1242–1244.

RESEARCH ARTICLE

AMERICAN JOURNAL OF medical genetics PART A

Submicroscopic Deletion in 7q31 Encompassing *CADPS2* and *TSPAN12* in a Child With Autism Spectrum Disorder and PHPV

Nobuhiko Okamoto,[1]* Yoshikazu Hatsukawa,[2] Keiko Shimojima,[3] and Toshiyuki Yamamoto[3]

[1]Department of Medical Genetics, Osaka Medical Center and Research Institute for Maternal and Child Health, Osaka, Japan

[2]Department of Ophthalmology, Osaka Medical Center and Research Institute for Maternal and Child Health, Osaka, Japan

[3]Institute for Integrated Medical Sciences, Tokyo Women's Medical University, Tokyo, Japan

Received 23 August 2010; Accepted 9 March 2011

We performed array comparative genomic hybridization utilizing a whole genome oligonucleotide microarray in a patient with the autism spectrum disorders (ASDs) and persistent hyperplastic primary vitreous (PHPV). Submicroscopic deletions in 7q31 encompassing *CADPS2* (Ca^{2+}-dependent activator protein for secretion 2) and *TSPAN12* (one of the members of the tetraspanin superfamily) were confirmed. The *CADPS2* plays important roles in the release of neurotrophin-3 and brain-derived neurotrophic factor. Mutations in *TSPAN12* are a relatively frequent cause of familial exudative vitreoretinopathy. We speculate that haploinsufficiency of *CADPS2* and *TSPAN12* contributes to ASDs and PHPV, respectively.

Key words: *CADPS2*; *TSPAN12*; autism; PHPV; CGH

How to Cite this Article:
Okamoto N, Hatsukawa Y, Shimojima K, Yamamoto T. 2011. Submicroscopic deletion in 7q31 encompassing *CADPS2* and *TSPAN12* in a child with autism spectrum disorder and PHPV.
Am J Med Genet Part A 155:1568–1573.

INTRODUCTION

Autism spectrum disorders (ASDs OMIM %209850) are complex neurodevelopmental conditions characterized by social communication disabilities, no or delayed language development, and stereotyped and repetitive behaviors. A number of studies have confirmed that genetic factors play an important role in ASDs.

About 10% of ASDs are associated with a Mendelian syndrome (e.g., fragile X syndrome, tuberous sclerosis and Timothy syndrome). Cytogenetic approaches revealed a high frequency of large chromosomal abnormalities (3–7% of patients), including the most frequently observed maternal 15q11-13 duplication (1–3% of patients). Association studies and mutation analysis of candidate genes have implicated the synaptic genes *NLGN3*(Neuroligin3 OMIM*300336), *NLGN4* (OMIM*300427) [Jamain et al., 2003], *SHANK3* (OMIM*606230)[Durand et al., 2007; Moessner et al., 2007], *NRXN1*(Neurexin1 MIM+600565) [Kim et al., 2008], *SHANK2* (OMIM*603290) [Berkel et al., 2010], and *CNTNAP2* (MIM*604569) [Alarcón et al., 2008; Arking et al., 2008] in ASDs. There is increasing evidence that the *SHANK3-NLGN4-NRNX1* postsynaptic density genes play important roles in the pathogenesis of ASDs.

Recently, on association between de novo copy number variation (CNV) and ASDs was revealed. Sebat et al. [2007] performed comparative genomic hybridization (CGH) on the genomic DNA from ASD patients and unaffected subjects to detect de novo CNV. As a result, they identified CNV in 12 out of 118 (10%) patients with sporadic ASD and confirmed de novo CNV were significantly associated with ASDs. Marshall et al. [2008] performed a genome-wide search for structural abnormalities in 427 unrelated ASD patients using SNP microarray analysis and karyotyping. De novo CNV were found in approximately 7% and approximately 2% of idiopathic families with one ASD child, or two or more ASD siblings, respectively. These authors discovered a CNV at 16p11.2 with an approximate frequency of 1%. Glessner et al. [2009] reported the results from a whole-genome CNV study of many European ASD patients and controls and found several new susceptibility genes encoding neuronal cell-adhesion molecules, including *NLGN1* and *ASTN2*, and genes involved in the ubiquitin pathways, including *UBE3A*, *PARK2*, *RFWD2*, and *FBXO40*. The investigators suggested that two gene networks, neuronal cell-

Grant sponsor: Ministry of Health, Labour and Welfare of Japan.
*Correspondence to:
Nobuhiko Okamoto, Department of Medical Genetics, Osaka Medical Center and Research Institute for Maternal and Child Health, 840 Murodo-cho, Izumi, Osaka 594-1101, Japan. E-mail: okamoto@osaka.email.ne.jp
Published online 27 May 2011 in Wiley Online Library (wileyonlinelibrary.com).
DOI 10.1002/ajmg.a.34028

adhesion and ubiquitin degradation, that are expressed within the central nervous system contribute to the genetic susceptibility of ASDs.

The International Molecular Genetic Study of Autism Consortium [1998] previously identified linkage loci on chromosomes 7 and 2, which were termed AUTS1 and AUTS5, respectively. Further genetic studies have provided evidence for AUTS1 being located on chromosome 7q [The International Molecular Genetic Study of Autism Consortium 2001]. Screening for mutations in six genes mapping to 7q, *CUTL1*, *SRPK2*, *SYPL*, *LAMB1*, *NRCAM*, and *PTPRZ1* in 48 unrelated individuals with autism led to the identification of several new coding variants in the *CUTL1*, *LAMB1*, and *PTPRZ1*genes [Bonora et al., 2005].

The human Ca^{2+}-dependent activator protein for secretion 2 (*CADPS2*: OMIM*609978) is also located on chromosome 7q31, which is within the AUTS1 locus [Cisternas et al., 2003]. It is a member of the CAPS/CADPS protein family that regulates the secretion of dense-core vesicles, which are abundant in the parallel fiber terminals of granule cells in the cerebellum and play important roles in the release of neurotrophin-3 (NT-3) and brain-derived neurotrophic factor (BDNF) [Sadakata et al., 2007a,b,c]. BDNF is indispensable for brain development and function, including the formation of synapses. Cisternas et al. [2003] studied *CADPS2* mutations in 90 unrelated autistic individuals, but identified no disease-specific variants. However, Sadakata et al. [2007a] reported that an aberrant, alternatively spliced *CADPS2* mRNA that lacks exon 3 (*CADPS2* Delta exon3) is detected in some patients with ASD.

Persistent hyperplastic primary vitreous (PHPV) is an ocular malformation caused by the presence of a retrolental fibrovascular membrane and the persistence of the posterior portion of the tunica vasculosa lentis and the hyaloid artery. It is often accompanied by microphthalmos, cataracts, and glaucoma. *NDP* (OMIM *300658, X-linked) and *FZD4* (OMIM *604579, dominant) were found to be mutated in unilateral and bilateral PHPV [Shastry, 2009]. These genes also cause Norrie disease and familial exudative vitreoretinopathy (FEVR), which share some clinical features with PHPV. FEVR is a genetically heterogeneous retinal disorder characterized by abnormal vascularization of the peripheral retina, which is often accompanied by retinal detachment. Mutations in the genes encoding *LRP5* (OMIM *603506, dominant and recessive) also cause FEVR. Junge et al. [2009] showed that *Tetraspanin12* (*Tspan12*) is expressed in the retinal vasculature, and loss of *Tspan12* phenocopies defects are seen in Fzd4, *Lrp5*, and *Norrin* mutant mice. *TSPAN12* is one of the members of the tetraspanin superfamily, characterized by the presence of four transmembrane domains. It constitutes large membrane complexes with other molecules. Nikopoulos et al. [2010] applied next-generation sequencing and found a mutation in *TSPAN12* (MIM*613168). Poulter et al. [2010] described seven mutations that were identified in a cohort of 70 FEVR patients without mutations in three known genes. Mutations in *TSPAN12*, which is at 7q31, are a relatively frequent cause of FEVR.

We performed array comparative genomic hybridization (array-CGH) utilizing a 44K whole genome oligonucleotide microarray in a patient with the ASDs and PHPV. Submicroscopic deletions in 7q31 encompassing *CADPS2* and *TSPAN12* were confirmed. We speculate that haploinsufficiency of *CADPS2* and *TSPAN12* contributes to ASD and PHPV, respectively.

CLINICAL REPORT

The patient, a 3-year-old boy, was born to nonconsanguineous healthy Japanese parents. His family history was unremarkable. He was born at 40 weeks' of gestation, his birth weight was 3,100 g, and his birth length was 50.0 cm. After birth, congenital nystagmus was noted, and he did not pursuit objects. An ophthalmological examination revealed bilateral PHPV. Cataract, glaucoma, and FEVR were not present. His gross motor development was normal, and his verbal development was delayed.

At 3 years of age, he came to our hospital for evaluation because of developmental delay. On examination dysmorphic features included a round face, low-set ears, broad eyebrows, apparent hypertelorism, blepharophimosis, hypoplastic alae nasi, a long philtrum, and a small mouth. His visual acuity was low, but he could perform daily activities with some support. In addition, impairment of social interaction, poor social skills, and strict adherence to routine behaviors were noted. He showed stereotypic movements and hyperactivity in his day care room. He was diagnosed as having an ASD according to the DSM-VI criteria. His DQ was 76 according to standard Japanese method. At 3 years and 8 months of age, his height, weight, and head circumference were 88.6 cm (−2.4 SD), 11.7 kg (−1.8 SD), and 46.8 cm (−2.4 S.D), respectively.

The results of routine laboratory tests were unremarkable. G-banded karyotype analysis revealed the following karyotype: 46,XY,inv(4)(p14;q21). Electroencephalography (EEG) showed occipital epileptic discharges. He was free from epileptic seizures.

Ultrasound evaluation revealed echogenic bands in the posterior segments of both globes. Magnetic resonance brain imaging also showed bilateral fibrous intraocular tissue (Fig. 1). However, no specific findings were found in the CNS including the cerebellum.

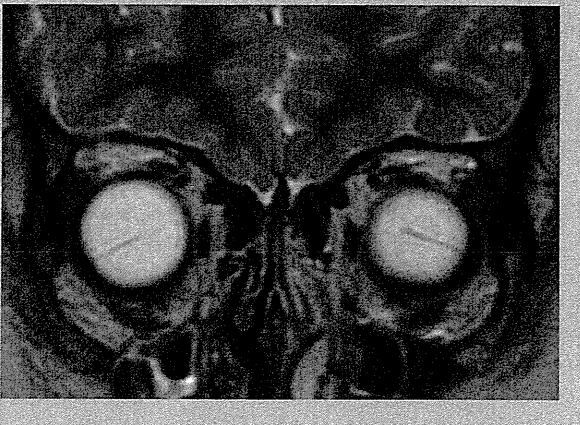

FIG. 1. MR coronal image, T2-weighted. Magnetic resonance imaging also showed fibrous intraocular tissue in the eye. [Color figure can be seen in the online version of this article, available at http://onlinelibrary.wiley.com/journal/10.1002/(ISSN)1552-4833]

MATERIALS AND METHODS

After obtaining informed consent based on a permission approved by the institution's ethical committee, peripheral blood samples were obtained from the patient and his parents. Genomic DNA was extracted using the QIAquick DNA extraction kit (QIAgen, Valencia, CA).

Array-CGH analysis was performed using the Human Genome CGH Microarray 44K (Agilent Technologies, Santa Clara, CA), as described previously [Shimojima et al., 2009].

Metaphase nuclei were prepared from peripheral blood lymphocytes using standard methods and were used for FISH analysis with human BAC clones selected from the UCSC genome browser (http://www.genome.ucsc.edu), as described elsewhere [Shimojima et al., 2009]. Physical positions refer to the March 2006 human reference sequence (NCBI Build 36.1).

RESULTS

Using array-CGH analysis, genomic copy number loss was identified in the 7q31.31 region (Fig. 2). The deletion was 5.4 Mb in size and included *CADPS2* and *TSPAN12*, but not *FOXP2*. There were no copy number changes in chromosome 4. FISH analyses confirmed the above deletion (Fig. 3). There were no deletions in either parent indicating de novo occurrence.

DISCUSSION

We described a patient with an ASD and PHPV who demonstrated submicroscopic deletion in chromosome 7q31.31. The deletion resides in the AUTS1 locus on chromosome 7q. The deleted region contained about 20 genes including *CADPS2* and *TSPAN12*. Little data are available about the association of other genes with developmental and ophthalmological disorders. We posit that haploinsufficiency of *CADPS2* and *TSPAN12* contributes to ASDs and PHPV, respectively.

Our patient fulfilled the DSM-VI criteria for an ASD. Poor eye contact, impairment of social interaction, poor social skills with strict adherence to routine, stereotypic movements, and hyperactivity were noted. However, his intellectual disability was mild. Ataxic movement was not observed.

There have been several reports of small deletions on chromosome 7q. Lennon et al. [2007] reported a young male with moderate intellectual disability, dysmorphic features, and language delay who had a deletion in the 7q31.1-7q31.31 region, which included the *FOXP2* gene. The patient demonstrated language impairment, including developmental verbal dyspraxia, but did not meet the criteria for autism. Cukier et al. [2009] reported a chromosomal inversion spanning the region from approximately 7q22.1 to 7q31 in autistic siblings. They suggested that an autism susceptibility gene is located in the chromosome 7q22–31 region. Dauwerse et al.

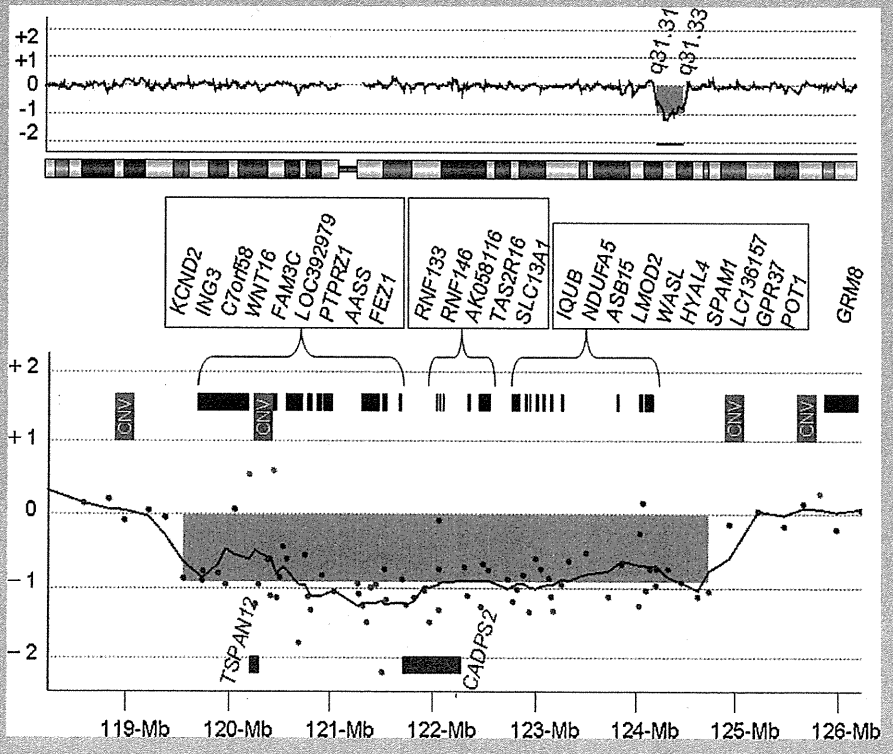

FIG. 2. Array-CGH of the patient. Loss of the genomic copy numbers was identified in the region of 7q31.31. The deletion size was 5.4 Mb and included *CADPS2* and *TSPAN12*.

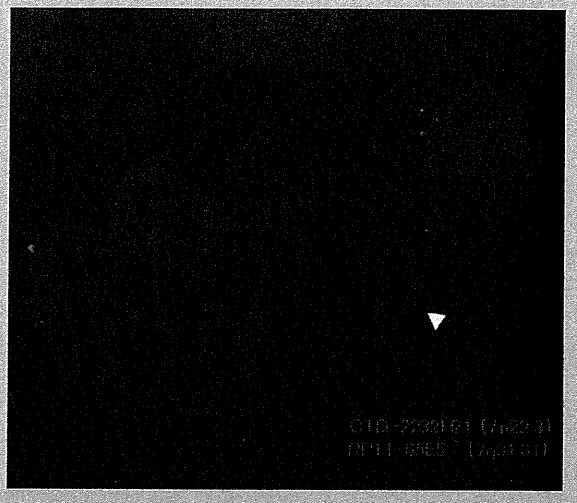

FIG. 3. FISH analyses of the patient. Arrow head indicates the deletion at 7q31.31.

[2010] characterized a de novo complex rearrangement of the long arm of chromosome 7 in a female patient with moderate mental retardation, anxiety disorder, and autistic features and suggested that disruption of the *C7orf58* gene contributed to the anxiety disorder, and autistic features of their patient. The *C7orf58* gene was also deleted in our patient. However, there have been no basic studies on the association of the *C7orf58* gene and brain function. Further studies are necessary on the role of the *C7orf58* gene.

Sadakata et al. [2007b] studied the behavior of *Cadps2−/−* mice. They showed impaired social interaction, hyperactivity, decreased exploratory behavior, and/or increased anxiety in a novel environment and deficits in intrinsic sleep–wake regulation and circadian rhythmicity. In addition, maternal neglect of newborns was a striking feature. They identified that *Cadps2−/−* mice show deficient release of NT-3 and BDNF. Cerebellar development was impaired in the mice. Sadakata et al. [2007a] found an aberrant alternatively spliced *CADPS2* mRNA that lacks exon 3 in some autistic patients. Exon 3 was shown to encode the dynactin 1-binding domain and affect axonal CADPS2 protein distribution. Exon 3-skipped CADPS2 protein possesses almost normal BDNF releasing activity but is not properly transported into the axons of neocortical or cerebellar neurons. However, Eran et al. [2009] observed no difference in prevalence of exon 3 skipping between ASDs and control samples. They concluded that exon 3 skipping represents a normal, minor isoform of CADPS2 in the cerebellum and is likely not a mechanism underlying autism susceptibility or pathogenesis. Our result may reinforce the evidence that *CADPS2* is associated with ASDs.

Cisternas et al. [2003] studied *CADPS2* gene mutations in 90 unrelated autistic individuals. However, they identified no disease-specific variants. Their results indicate that *CADPS2* mutations are not a major cause of ASDs. However, although small deletions of *CADPS2* as found in the present patient, might be rare, they support the idea that *CADPS2* abnormalities are associated with autism susceptibility.

Nikopoulos et al. [2010] reported two missense mutations in five of 11 FEVR families, indicating that mutations in *TSPAN12* are a relatively frequent cause of FEVR. Both residues are completely conserved throughout vertebrate evolution. These authors suggested that both haploinsufficiency and a dominant-negative effect of the mutant TSPAN12 on the wild-type protein should be considered as underlying disease mechanisms. Poulter et al. [2010] described mutations in the *TSPAN12* gene in FEVR patients and suggested that haploinsufficiency of *TSPAN12* causes FEVR because at least four of the seven mutations are predicted to lead to transcripts with premature-termination codons that are likely to be targeted by nonsense-mediated decay.

Recently, the Norrin/Frizzled4 signaling pathway that acts on the on the surface of developing endothelial cells and controls retinal vascular development is highlighted [Ye et al., 2010]. This pathway is composed of Norrin, its transmembrane receptor, Frizzled4, coreceptor, Lrp5, and an auxiliary membrane protein, Tspan12. The resulting signal controls a transcriptional program that regulates endothelial growth and maturation. PHPV and FEVR are associated with their pathogenesis. Our findings indicate that haploinsufficiency of *TSPAN12* is a plausible causative mechanism for PHPV. It will be interesting to study *TSPAN12* abnormalities in PHPV without *NDP* and *FZD4* mutations.

Singh et al. [2006] reported a voltage-gated potassium channel gene mutation in a temporal lobe epilepsy patient, namely a Kv4.2 truncation mutation lacking the last 44 amino acids in the carboxyl terminal. Kv4.2 channel is encoded by the *KCND2* gene. We suggest that the epileptic discharges on EEG reflect neuronal excitability caused by haploinsufficiency of *KCND2*.

Shen et al. [2010] suggested that using chromosomal microarray analysis to test for submicroscopic genomic deletions and duplications should be considered as part of the initial diagnostic evaluation of patients with ASDs. Miller et al. [2010] suggested that the use of chromosomal microarray is recommended as the first-tier cytogenetic diagnostic test for patients with unexplained developmental delay/intellectual disability, ASDs, or multiple congenital anomalies. In patients with ASDs and other anomalies, chromosomal microarray may be the useful method to clarify the underlying defect.

ACKNOWLEDGMENTS

We thank the patient's family for their cooperation. This study was supported by Health and Labour Research Grants from the Ministry of Health, Labour and Welfare of Japan.

REFERENCES

Alarcón M, Abrahams BS, Stone JL, Duvall JA, Perederiy JV, Bomar JM, Sebat J, Wigler M, Martin CL, Ledbetter DH, Nelson SF, Cantor RM, Geschwind DH. 2008. Linkage, association, and gene-expression analyses identify CNTNAP2 as an autism-susceptibility gene. Am J Hum Genet 82:150–159.

Arking DE, Cutler DJ, Brune CW, Teslovich TM, West K, Ikeda M, Rea A, Guy M, Lin S, Cook EH, Chakravarti A. 2008. A common genetic variant in the neurexin superfamily member CNTNAP2 increases familial risk of autism. Am J Hum Genet 82:160–164.

Berkel S, Marshall CR, Weiss B, Howe J, Roeth R, Moog U, Endris V, Roberts W, Szatmari P, Pinto D, Bonin M, Riess A, Engels H, Sprengel R, Scherer SW, Rappold GA. 2010. Mutations in the SHANK2 synaptic scaffolding gene in autism spectrum disorder and mental retardation. Nat Genet 42:489–491.

Bonora E, Lamb JA, Barnby G, Sykes N, Moberly T, Beyer KS, Klauck SM, Poustka F, Bacchelli E, Blasi F, Maestrini E, Battaglia A, Haracopos D, Pedersen L, Isager T, Eriksen G, Viskum B, Sorensen EU, Brondum-Nielsen K, Cotterill R, Engeland H, Jonge M, Kemner C, Steggehuis K, Scherpenisse M, Rutter M, Bolton PF, Parr JR, Poustka A, Bailey AJ, Monaco AP, International Molecular Genetic Study of Austism Consortium. 2005. Mutation screening and association analysis of six candidate genes for autism on chromosome 7q. Eur J Hum Genet 13:198–207.

Cisternas FA, Vincent JB, Scherer SW, Ray PN. 2003. Cloning and characterization of human CADPS and CADPS2, new members of the Ca^{2+}-dependent activator for secretion protein family. Genomics 81: 279–291.

Cukier HN, Skaar DA, Rayner-Evans MY, Konidari I, Whitehead PL, Jaworski JM, Cuccaro ML, Pericak-Vance MA, Gilbert JR. 2009. Identification of chromosome 7 inversion breakpoints in an autistic family narrows candidate region for autism susceptibility. Autism Res 2: 258–266.

Dauwerse JG, Ruivenkamp CA, Hansson K, Marijnissen GM, Peters DJ, Breuning MH, Hilhorst-Hofstee Y. 2010. A complex chromosome 7q rearrangement identified in a patient with mental retardation, anxiety disorder, and autistic features. Am J Med Genet Part A 152A:427–433.

Durand CM, Betancur C, Boeckers TM, Bockmann J, Chaste P, Fauchereau F, Nygren G, Rastam M, Gillberg IC, Anckarsäter H, Sponheim E, Goubran-Botros H, Delorme R, Chabane N, Mouren-Simeoni MC, de Mas P, Bieth E, Rogé B, Héron D, Burglen L, Gillberg C, Leboyer M, Bourgeron T. 2007. Mutations in the gene encoding the synaptic scaffolding protein SHANK3 are associated with autism spectrum disorders. Nat Genet 39:25–27.

Eran A, Graham KR, Vatalaro K, McCarthy J, Collins C, Peters H, Brewster SJ, Hanson E, Hundley R, Rappaport L, Holm IA, Kohane IS, Kunkel LM. 2009. Comment on "Autistic-like phenotypes in Cadps2-knockout mice and aberrant CADPS2 splicing in autistic patients". J Clin Invest 119: 679–680.

Glessner JT, Wang K, Cai G, Korvatska O, Kim CE, Wood S, Zhang H, Estes A, Brune CW, Bradfield JP, Imielinski M, Frackelton EC, Reichert J, Crawford EL, Munson J, Sleiman PM, Chiavacci R, Annaiah K, Thomas K, Hou C, Glaberson W, Flory J, Otieno F, Garris M, Soorya L, Klei L, Piven J, Meyer KJ, Anagnostou E, Sakurai T, Game RM, Rudd DS, Zurawiecki D, McDougle CJ, Davis LK, Miller J, Posey DJ, Michaels S, Kolevzon A, Silverman JM, Bernier R, Levy SE, Schultz RT, Dawson G, Owley T, McMahon WM, Wassink TH, Sweeney JA, Nurnberger JI, Coon H, Sutcliffe JS, Minshew NJ, Grant SF, Bucan M, Cook EH, Buxbaum JD, Devlin B, Schellenberg GD, Hakonarson H. 2009. Autism genome-wide copy number variation reveals ubiquitin and neuronal genes. Nature 459:569–573.

International Molecular Genetic Study of Autism Consortium. 1998. A full genome screen for autism with evidence for linkage to a region on chromosome 7q. Hum Mol Genet 7:571–578.

International Molecular Genetic Study of Autism Consortium (IMGSAC). 2001. Further characterization of the autism susceptibility locus AUTS1 on chromosome 7q. Hum Mol Genet 10:973–982.

Jamain S, Quach H, Betancur C, Råstam M, Colineaux C, Gillberg IC, Soderstrom H, Giros B, Leboyer M, Gillberg C, Bourgeron T. Paris Autism Research International Sibpair Study. 2003. Mutations of the X-linked genes encoding neuroligins NLGN3 and NLGN4 are associated with autism. Nat Genet 34:27–29.

Junge HJ, Yang S, Burton JB, Paes K, Shu X, French DM, Costa M, Rice DS, Ye W. 2009. TSPAN12 regulates retinal vascular development by promoting Norrin- but not Wnt-induced FZD4/beta-catenin signaling. Cell 139:299–311.

Kim HG, Kishikawa S, Higgins AW, Seong IS, Donovan DJ, Shen Y, Lally E, Weiss LA, Najm J, Kutsche K, Descartes M, Holt L, Braddock S, Troxell R, Kaplan L, Volkmar F, Klin A, Tsatsanis K, Harris DJ, Noens I, Pauls DL, Daly MJ, MacDonald ME, Morton CC, Quade BJ, Gusella JF. 2008. Disruption of neurexin 1 associated with autism spectrum disorder. Am J Hum Genet 82:199–207.

Lennon PA, Cooper ML, Peiffer DA, Gunderson KL, Patel A, Peters S, Cheung SW, Bacino CA. 2007. Deletion of 7q31.1 supports involvement of FOXP2 in language impairment: Clinical report and review. Am J Med Genet A 143A:791–798.

Marshall CR, Noor A, Vincent JB, Lionel AC, Feuk L, Skaug J, Shago M, Moessner R, Pinto D, Ren Y, Thiruvahindrapduram B, Fiebig A, Schreiber S, Friedman J, Ketelaars CE, Vos YJ, Ficicioglu C, Kirkpatrick S, Nicolson R, Sloman L, Summers A, Gibbons CA, Teebi A, Chitayat D, Weksberg R, Thompson A, Vardy C, Crosbie V, Luscombe S, Baatjes R, Zwaigenbaum L, Roberts W, Fernandez B, Szatmari P, Scherer SW. 2008. Structural variation of chromosomes in autism spectrum disorder. Am J Hum Genet 82:477–488.

Miller DT, Adam MP, Aradhya S, Biesecker LG, Brothman AR, Carter NP, Church DM, Crolla JA, Eichler EE, Epstein CJ, Faucett WA, Feuk L, Friedman JM, Hamosh A, Jackson L, Kaminsky EB, Kok K, Krantz ID, Kuhn RM, Lee C, Ostell JM, Rosenberg C, Scherer SW, Spinner NB, Stavropoulos DJ, Tepperberg JH, Thorland EC, Vermeesch JR, Waggoner DJ, Watson MS, Martin CL, Ledbetter DH. 2010. Consensus statement: Chromosomal microarray is a first-tier clinical diagnostic test for individuals with developmental disabilities or congenital anomalies. Am J Hum Genet 86:749–764.

Moessner R, Marshall CR, Sutcliffe JS, Skaug J, Pinto D, Vincent J, Zwaigenbaum L, Fernandez B, Roberts W, Szatmari P, Scherer SW. 2007. Contribution of SHANK3 mutations to autism spectrum disorder. Am J Hum Genet 81:1289–1297.

Nikopoulos K, Gilissen C, Hoischen A, van Nouhuys CE, Boonstra FN, Blokland EA, Arts P, Wieskamp N, Strom TM, Ayuso C, Tilanus MA, Bouwhuis S, Mukhopadhyay A, Scheffer H, Hoefsloot LH, Veltman JA, Cremers FP, Collin RW. 2010. Next-generation sequencing of a 40 Mb linkage interval reveals TSPAN12 mutations in patients with familial exudative vitreoretinopathy. Am J Hum Genet 86:240–247.

Poulter JA, Ali M, Gilmour DF, Rice A, Kondo H, Hayashi K, Mackey DA, Kearns LS, Ruddle JB, Craig JE, Pierce EA, Downey LM, Mohamed MD, Markham AF, Inglehearn CF, Toomes C. 2010. Mutations in TSPAN12 cause autosomal-dominant familial exudative vitreoretinopathy. Am J Hum Genet 86:248–253.

Sadakata T, Washida M, Iwayama Y, Shoji S, Sato Y, Ohkura T, Katoh-Semba R, Nakajima M, Sekine Y, Tanaka M, Nakamura K, Iwata Y, Tsuchiya KJ, Mori N, Detera-Wadleigh SD, Ichikawa H, Itohara S, Yoshikawa T, Furuichi T. 2007a. Autistic-like phenotypes in Cadps2-knockout mice and aberrant CADPS2 splicing in autistic patients. J Clin Invest 117:931–943.

Sadakata T, Kakegawa W, Mizoguchi A, Washida M, Katoh-Semba R, Shutoh F, Okamoto T, Nakashima H, Kimura K, Tanaka M, Sekine Y, Itohara S, Yuzaki M, Nagao S, Furuichi T. 2007b. Impaired cerebellar development and function in mice lacking CAPS2, a protein involved in neurotrophin release. J Neurosci 27:2472–2482.

Sadakata T, Washida M, Furuichi T. 2007c. Alternative splicing variations in mouse CAP S2: Differential expression and functional properties of splicing variants. BMC Neurosci 8:25.

Sebat J, Lakshmi B, Malhotra D, Troge J, Lese-Martin C, Walsh T, Yamrom B, Yoon S, Krasnitz A, Kendall J, Leotta A, Pai D, Zhang R, Lee YH, Hicks

J, Spence SJ, Lee AT, Puura K, Lehtimäki T, Ledbetter D, Gregersen PK, Bregman J, Sutcliffe JS, Jobanputra V, Chung W, Warburton D, King MC, Skuse D, Geschwind DH, Gilliam TC, Ye K, Wigler M. 2007. Strong association of de novo copy number mutations with autism. Science 316:445–449.

Shastry BS. 2009. Persistent hyperplastic primary vitreous: Congenital malformation of the eye. Clin Experiment Ophthalmol 37:884–890.

Shen Y, Dies KA, Holm IA, Bridgemohan C, Sobeih MM, Caronna EB, Miller KJ, Frazier JA, Silverstein I, Picker J, Weissman L, Raffalli P, Jeste S, Demmer LA, Peters HK, Brewster SJ, Kowalczyk SJ, Rosen-Sheidley B, McGowan C, Duda AW III, Lincoln SA, Lowe KR, Schonwald A, Robbins M, Hisama F, Wolff R, Becker R, Nasir R, Urion DK, Milunsky JM, Rappaport L, Gusella JF, Walsh CA, Wu BL, Miller DT. Autism Consortium Clinical Genetics/DNA Diagnostics Collaboration. 2010. Clinical genetic testing for patients with autism spectrum disorders. Pediatrics 125:e727–e735.

Shimojima K, Páez MT, Kurosawa K, Yamamoto T. 2009. Proximal interstitial 1p36 deletion syndrome: The most proximal 3.5-Mb microdeletion identified on a dysmorphic and mentally retarded patient with inv(3)(p14.1q26.2). Brain Development 31:629–633.

Singh B, Ogiwara I, Kaneda M, Tokonami N, Mazaki E, Baba K, Matsuda K, Inoue Y, Yamakawa K. 2006. A Kv4.2 truncation mutation in a patient with temporal lobe epilepsy. Neurobiol Dis 24:245–253.

Ye X, Wang Y, Nathans J. 2010. The Norrin/Frizzled4 signaling pathway in retinal vascular development and disease. Trends Mol Med 16:417–425.